Published in final edited form as:
J Neurochem. 2012 March ; 120(6): 974–984. doi:10.1111/j.1471-4159.2012.07651.x.

GROUP IVA PHOSPHOLIPASE A_2 IS NECESSARY FOR GROWTH CONE REPULSION AND COLLAPSE

Staci D. Sanford[1], **Bo Goen Yun**[2], **Christina C. Leslie**[2], **Robert C. Murphy**[3], and **Karl H. Pfenninger**[1]

[1]Department of Pediatrics, Neuroscience Program, and Colorado Intellectual and Developmental Disabilities Research Center, University of Colorado School of Medicine, Aurora, CO, 80045

[2]Department of Pediatrics, National Jewish Health, Denver, CO, 80206 and Departments of Pathology and Pharmacology, University of Colorado School of Medicine, Aurora, CO, 80045

[3]Department of Pharmacology, University of Colorado School of Medicine, Aurora, CO, 80045

Abstract

The repellent semaphorin 3A (Sema3A) causes growth cone turning or collapse by triggering cytoskeletal rearrangements and detachment of adhesion sites. Growth cone detachment is dependent on eicosanoid activation of protein kinase C epsilon (PKCε), but the characterization of the phospholipase A_2 (PLA_2) that releases arachidonic acid (AA) for eicosanoid synthesis has remained elusive. Here we show in rat dorsal root ganglion neurons that Sema3A stimulates PLA_2 activity, that Sema3A-induced growth cone turning and collapse are dependent on the release of AA, and that the primary PLA_2 involved is the Group IV α isoform (GIVA). Silencing GIVA expression renders growth cones resistant to Sema3A-induced collapse, and GIVA inhibition reverses Sema3A-induced repulsion into attraction. These studies identify a novel, early step in Sema3A-signaling and a PLA_2 necessary for growth cone repulsion and collapse.

Keywords

Axonal growth cone; phospholipase A_2; growth cone repulsion; signaling

Axons have amoeboid tips, termed growth cones, that navigate to the correct targets as they advance. This process is fundamental to the establishment of neuronal circuitry. Axonal growth cones are able to respond to numerous molecular signals, and their integration translates into changes in direction and speed. The molecular mechanisms that direct these responses are complex and require strict temporal and spatial regulation of adhesion and the cytoskeleton (Lauffenburger and Horwitz, 1996; Suter and Forscher, 2000).

Repellent gradients cause negative chemotaxis of the growth cone. This requires cytoskeletal rearrangement and disassembly, as well as localized detachment of adhesion sites from the growth substratum (Gatlin et al., 2006; Liu and Strittmatter, 2001; Mikule et al., 2002). When uniformly applied, repellents cause more extensive growth cone detachment and collapse (Fan and Raper, 1995; Luo et al., 1993; Mikule et al., 2002). The repellents semaphorin 3A (Sema3A) and thrombin trigger dissociation of growth cone adhesion sites via signaling that involves synthesis of the eicosanoid 12(S)-hydroxyeicosatetraenoic acid [12(S)-HETE] from free arachidonic acid (AA). 12(S)-HETE

Address correspondence to: Karl H. Pfenninger, MD, Department of Pediatrics, University of Colorado School of Medicine, Aurora, CO, 80045, Phone: 303-724-3466; fax 303-724-3838, Karl.Pfenninger@ucdenver.edu.

directly activates protein kinase C epsilon [PKCε; (Mikule et al., 2002; Mikule et al., 2003)], whose primary target is the myristoylated, alanine-rich C-kinase substrate (MARCKS), an adhesion-associated protein (Gatlin et al., 2006; Kim et al., 1994; Mikule et al., 2003). Upon phosphorylation, MARCKS moves from adhesions into the cytosol (Gatlin et al., 2006; Kim et al., 1994; Thelen et al., 1991). This was borne out by functional studies, which have shown that 12(S)-HETE synthesis, PKC activation, and MARCKS phosphorylation are all necessary and sufficient for growth cone detachment, turning and collapse (Gatlin et al., 2006; Mikule et al., 2002; Mikule et al., 2003).

Free AA is generated by phospholipase A_2 (PLA_2; EC3.1.1.4), which hydrolyzes phospholipids at their sn-2 position. PLA_2s fall into two classes, secreted and intracellular. These classes can be broken down further into ten groups of secreted PLA_2s [$sPLA_2$; (Murakami and Kudo, 2004)] and two groups of intracellular PLA_2s: Group VI (GVI), which are calcium-independent, and Group IV (GIV), most of which are calcium-dependent (except for GIVC). These groups are also referred to as $iPLA_2$ and $cPLA_2$, respectively, and each constitutes a family of several isoenzymes [for reviews see (Ghosh et al., 2006; Schaloske and Dennis, 2006)]. Previous data indicate growth cones contain two cytosolic high-molecular-weight forms of PLA_2 (Negre-Aminou et al., 1996). We have shown that thrombin stimulates PLA_2 and increases free AA and 12(S)-HETE in isolated growth cones (de la Houssaye et al., 1999), but this has not been shown for Sema3A. In neither case was the participating PLA_2 characterized. The present study establishes in rat dorsal root ganglion (DRG) neurons that GIVA PLA_2 (GIV α isoform, also referred to as $cPLA_2\alpha$) is activated by Sema3A and is necessary for Sema3A-induced growth cone turning and collapse.

Experimental Procedures

Materials

Reagents and their sources were: Nerve growth factor (NGF), Alomone Labs (Jerusalem, Israel); culture media, medium supplements, laminin, “Stealth Select RNAi” siRNA duplex oligoribonucleotides, SlowFade Gold antifade reagent, and Cy5-conjugated secondary antibody, Life Technologies/Invitrogen Co. (Carlsbad, CA); fetal bovine serum (FBS), HyClone (Logan, UT); 12(S)-hydroxyeicosatetraenoic acid [12(S)-HETE], arachidonyltrifluoromethyl ketone ($AACOCF_3$), and racemic bromoenol lactone (BEL), Biomol International, L.P. (Plymouth Meeting, PA); N-{(2S,4R)-4-(Biphenyl-2-ylmethyl-isobutyl-amino)-1-[2-(2,4-difluorobenzoyl)-benzoyl]-pyrrolidin-2-ylmethyl}-3-[4-(2,4-dioxothiazolidin-5-ylidenemethyl)-phenyl]acrylamide (pyrrolidine), EMD Biosciences/ Calbiochem (San Diego, CA); Wyeth-1, gift from Dr. M. Gelb (University of Washington, Seattle, Washington). Eicosanoid and deuterated internal standards for mass spectrometry ([d_8]-12(S)-HETE, ≥ 99 atom %d; and [d_8]-arachidonic acid, ≥ 96 atom %d) were from Cayman Chemical Co. (Ann Arbor, MI). All other chemicals (highest quality available), Fisher Scientific (Waltham, MA) or Sigma (St Louis, MO). Sema3A- The culture supernatant of stably transfected HEK 293 cells secreting Sema3A (gift of Dr. M. Tessier-Lavigne) was concentrated by ultrafiltration (Centriplus membrane, 50,000 MW cut-off; Millipore Co., Bedford, MA) and calibrated by bioassay, so as to trigger growth cone collapse within fifteen min (Gatlin et al., 2006). The appropriate control was identically processed and diluted supernatant of HEK293 cells transfected with empty vector (pCEP4). For the PLA_2 activation experiments we used highly purified recombinant Sema3A-Fc chimera from R&D systems (Minneapolis, MN).

Growth Cone Isolation

Growth cones ("growth cone particles", GCPs) were isolated from day 18 fetal rat brains (Sprague-Dawley) as described previously (Lohse et al., 1996; Pfenninger et al., 1983). The GCP fraction, collected at the 0.32/0.83M sucrose interface, was diluted with 5–10 volumes 0.32M sucrose containing 1mM $MgCl_2$, 2mM TES, pH 7.3, pelleted (40,000*g* for 30 min), and then resuspended and used for the experiments.

DRG Neuron Culture

DRGs were dissected from the whole length of the spinal cord, from 15-day gestation Sprague-Dawley rat fetus, and cultured on laminin-coated coverslips (Assistent brand) in Neurobasal medium supplemented with B27, 10% v/v FBS and 100ng/ml NGF (3.8nM). After 24h incubation (37°C, 5% CO_2 in air) this medium was replaced with fresh Neurobasal medium plus B27, without other supplementation. After a second day in culture, neurites with spread growth cones were used for collapse or turning assays. For biochemical studies and experiments involving transfection DRGs were dissociated with trypsin/EDTA prior to electroporation and/or plating. Cells were counted with a hemocytometer. Culture conditions were the same as those for explants.

Phospholipase A_2 assays

PLA_2 activity was measured as release of AA and eicosanoid in DRG cultures. Equal aliquots of cell suspension (approximately 5×10^5 dissociated DRG neurons) were plated on laminin-coated coverslips (25mm diameter). Dishes with coverslip, but without cells, served to determine background. Approximately 24hrs after plating, cultures were changed twice (1 hour each) to 0.9ml fresh pre-warmed Neurobasal medium with 0.1% fatty-acid-free bovine serum albumin (BSA) and B27. Challenge media (100µl) were introduced into the cultures for 6min at 37°C before the reaction was stopped. The final Sema3A-Fc concentration was 100ng/ml. To stop the reaction dishes were placed onto an ice-cold metal plate. Culture supernatant was removed immediately and collected in tubes containing 1ml ice-cold methanol.

Culture supernatants were first diluted to 80% methanol to precipitate proteins, and internal standards (1 ng each) were added. This solution, diluted with water to <15% methanol, was loaded on a solid phase extraction cartridge (Strata Polymeric Reversed Phase 60mg/1ml; Phenomenex, Torrance, CA) that was first flushed with 10 ml water and then with 1 ml methanol to elute the eicosanoids. This eluate was dried down and reconstituted in 75µl of HPLC solvent A (8.3 mM acetic acid buffered to pH 5.7 with NH_4OH) and 25 µl of solvent B (CH_3CN/CH_3OH, 65/35, v/v).

Metabolite separation and mass spectrometry: Sample aliquots (50 µl) were injected into an HPLC system for eicosanoid separation on a C18 reversed-phase column (Ascentis 15cm × 2.1mm, 5µm particle size, Supelco), eluted at a flow rate of 200µl/min with a solvent A/B gradient from 25% to 60% in 8 min, then B increased to 75% in 5 min, 80% in 7 min, 98% in 2 min, and held for 4 min. The HPLC system was interfaced with the electrospray source of a triple quadrupole mass spectrometer (Sciex API 3000, PE-Sciex, Thronhill Ontario, Canada), where analyses were performed in negative-ion mode using multiple reaction monitoring (MRM) of the specific transitions: [d_8]-arachidonic acid *m/z* 311→ 267, [d_8]-12(S)-HETE *m/z* 327→ 184, 12-HETE *m/z* 319 →179, and arachidonic acid *m/z* 303→259. Quantitation was performed using a standard isotope dilution curve as described (Hall, 1998).

Growth Cone Collapse Assays

DRG cultures on laminin-coated coverslips were placed in an Attofluor cell chamber (Molecular Probes/Invitrogen, Carlsbad, CA) with medium, and layered-over with inert mineral oil (embryo-tested, sterile-filtered; Sigma, St Louis, MO) to maintain pH and avoid evaporation. During observation on the microscope stage, with convective heating at 37°C, cultures were challenged with either pCEP4 or Sema3A and phase contrast images were acquired. Growth cone collapse was quantified by measuring the total area of the same live growth cone, determined with the tracing function in Image J software (National Institutes of Health), before and after treatment.

Growth cone turning assays

Sema3A gradients were generated in the proximity of nerve growth cones by repetitive-pulse application (Lohof et al., 1992), exactly as described (Sanford et al, 2008). Culture coverslips were placed on the microscope stage as indicated above. At the start of each experiment, the micropipette tip was positioned 100μm away from the selected growth cone, at an angle of 45° relative to the initial direction of growth cone advance (orientation of the neurite shaft). Prior to onset of factor expulsion growth cones were monitored for 15 min. Initiation of factor expulsion marked the start (time t=0) for each experiment. Phase contrast images were captured at 5-min intervals for 1h. To be scored, growth cones had to advance ≥10μm during the assay and were tracked for 1h or until they either stopped (i.e., no advancement for ≥ 10 min) or branched. Turning angles were the angles between the initial axis of outgrowth and a line drawn from the initial to the final position of the growth cone (Gatlin et al., 2006; Sanford, 2008).

siRNA Knockdown of GIVA

Dissociated DRG cells ($2–3\times10^6$) were pelleted and resuspended in 100μl Nucleofector solution (Amaxa, Gaithersburg, MD) with 10nM each of three different rat GIVA-targeted siRNAs plus 1.5μg of pmaxGFP (Amaxa), and electroporated using the Amaxa Nucleofector device (setting O-003). The siRNAs (Stealth Select RNAi; Life Technologies/ Invitrogen Co., Carlsbad, CA) were:

NM_133551.1-1551 RSS302598 5′-ACCAAGCAAGTTGGGTCCATCGGAT-3′;

NM_133551.1-2344 RSS302599 5′-TCGTTGCTCTGTTTCCCTCAGTAAT-3′

NM_133551.1-1739 RSS302600 5′-GCAGCGGTAGCAGATCCAGATGAAT-3′

Transfected neurons were cultured on laminin as described above.

GIVA knockdown controls were performed with immortalized mouse lung fibroblasts (IMLF), generated and cultured as described previously (Stewart et al., 2002). Cells were transfected with the mixture of siRNA duplexes to rat GIVA (see above), a single stealth siRNA duplex to mouse PLA2G4A (NM_008869 MSS276366 5′-CCCAGGUGUUCUAAGGGAAACCAAA-3′), or stealth siRNA negative control (12935–300, Invitrogen). After transfection with oligofectamine 2000 (Invitrogen), cells were incubated for 48 hr, RNA was isolated (RNeasy Mini Kit, Qiagen), and 1μg of total RNA was used for cDNA synthesis with random hexamer primers (Superscript III polymerase, Invitrogen). Real-time qPCR was performed using TaqMan fast universal PCR master mix on the StepOne Plus real-time PCR system (Applied Biosystems). TaqMan Assay probes used were: Mm 01284326_m1 (PLA2GIVA), Mm 01271079_m1 (PLA2GIVB, $cPLA_2\beta$), Mm 01279432_g1 (PLA2GIVE, $cPLA_2\varepsilon$) and Mm 01338178_m1 (PLA2GIVF, $cPLA_2\zeta$) (Ghosh et al., 2007). The housekeeping gene β-glucuronidase was used for normalization. Real time qPCR reaction conained 10μl 2x TaqMan fast universal master mix, 1μl 20x TaqMan Assay/probe and 9μl of 75–100ng cDNA in RNase-free water. Thermal Fast cycle

program was: 20s at 95°C followed by 40 cycles of 1s at 95°C and 20s at 60°C. Triplicate reactions were analyzed for each sample. Threshold cycle values (C_T) were determined and used for $2^{-\Delta\Delta C}$T analysis of gene expression (Livak and Schmittgen, 2001).

Knockdown of GIVA PLA_2 protein in neurons could not be assessed by Western blot because of low transfection efficiency (~30%) but was shown by immunocytochemistry and densitometry. Analyses were performed using the spot densitometry function of Alphaease software (Alpha Innotech, San Leandro, CA).

Fixation and Labeling of Growth Cones in Culture

DRG cultures were fixed using slow infusion of 4% (wt/vol) formaldehyde in 0.1M phosphate buffer, pH 7.4, with 120mM glucose and 0.4mM $CaCl_2$ (Pfenninger and Maylie-Pfenninger, 1981). Cultures were rinsed (three times) with phosphate-buffered saline (PBS) containing 1mM glycine, permeabilized with 1% (vol/vol) Brij98 detergent in blocking buffer [PBS, 5% goat serum, and 3% (wt/vol) BSA] for 2 min, and placed in blocking buffer for 1 h (all at room temperature). Quenched cultures were incubated with primary antibody (1:1000 dilution in blocking buffer), over night at 4°C, and washed (3x) with blocking buffer. The GIVA antibody was localized with the Vectastain ABC kit (Vector Laboratories, Burlingame, CA). Coverslips were mounted on slides with SlowFade Gold antifade reagent.

Microscopy

All images were captured using a Zeiss Axiovert 200M microscope equipped with Zeiss optics, Cooke Sensicam camera, and Metamorph software (Molecular Devices Co., Sunnyvale, CA).

Gel Electrophoresis and Western Analysis

Polypeptides were resolved by SDS-PAGE along with Precision Plus protein standards (Bio-Rad, Hercules, CA) and electrotransferred (Towbin et al., 1979) onto Immobilon P (Millipore, Billercia, MA) membranes. Blots were blocked in Tris-buffered saline (TBS) with 5% non-fat evaporated milk and 0.1% Tween-20 overnight at 4°C. After quenching, blots were incubated in blocking buffer containing GIVA PLA_2 primary antibody (de Carvalho et al., 1993) for 1 h, rinsed in blocking buffer (three times), and incubated with Cy5-conjugated secondary antibody in blocking buffer. After three rinses in TBS/Tween, blots were scanned (Typhoon 9400 imager; GE Healthcare, Pittsburgh, PA).

Statistical Analyses

Data are presented as means ± standard errors. Normality of all variables was examined using both Shapiro-Wilk and Kolmogorov-Smirnov tests. For data that were not normally distributed, the Kruskal-Wallis (K-W) test was used to compare different conditions. To determine which pairs of conditions were different under the K-W test, the Dunn procedure was used. When the data were normal, we applied analysis of variance (ANOVA), combined with False Discovery Rate (FDR) methods, to correct for multiple comparisons with 5% experiment-wise type I error rate. All statistical comparisons were carried out using SAS® release 9.2 (SAS Institute Inc., Cary, NC). The data shown in Figures 1 and 5 were normally distributed. The data distributions in Figures 2 and 4 were marginally normal. Therefore, we indicated the results of both ANOVA and K-W analyses.

Results

Sema3A increases AA and derivatives in DRG cultures

Our earlier work demonstrated in GCPs that the repellent thrombin stimulates PLA_2 activity and the release of free AA (de la Houssaye et al., 1999). We also showed that, relative to fetal brain homogenate, GCPs are highly enriched in PLA_2 activity, and that GCP cytosol contains at least two types of PLA_2 of high molecular mass that are active in low- or no-calcium environments (Negre-Aminou et al., 1996). This suggested the involvement of GIV or GVI PLA_2 in AA release stimulated by thrombin and, possibly, Sema3A. Dorsal root ganglion (DRG) neurons cultured in the presence of NGF express NP-1 (Mikule et al., 2002) and are a well-established system for investigating Sema3A-induced growth cone turning or collapse (Gatlin et al., 2006; Song et al., 1998). Although they are challenging for biochemical experiments (limited number of neurons; fragility of neurite outgrowth) we were able to measure AA and eicosanoid release in culture supernatants using mass spectrometry.

To determine whether Sema3A increased release of AA and its HETE derivatives, we compared supernatants of Sema3A- and vehicle-challenged (6 min) cultures of dissociated, growing DRG neurons (Fig. 1). We used highly purified Sema3A-Fc chimera protein for challenge. Sema3A Fc significantly stimulated AA release relative to control, from 39.8 ± 2.27 to 58.5 ± 5.22 ng AA/culture (mean ± s.e.m.; n = 4; $p < 0.01$ in two-sample t-test; corresponding power, 88.2%). Thus, Sema3A increases PLA_2 activity in DRG cultures. Sema3A challenge also increased the level of 12-HETE over 5-fold, to 0.86±0.07 ng/culture from 0.17±0.02 ng/culture for vehicle challenge ($p \leq 0.0005$; ANOVA FDR; n=3). It elicited smaller but significant increases for 15-HETE and 5-HETE (data not shown). The dominant HETE species was 12-HETE, but its stimulated level was only about 1% of that of free AA (note different scales in Fig. 1).

Effects of different PLA_2 inhibitors on Sema3A-induced growth cone collapse

If Sema3A activation of a specific PLA_2 is necessary for the repellent response, inhibition of that, but not of other PLA_2s, should block the response. This was tested with various PLA_2 inhibitors in collapse assays of DRG growth cones using uniform (bath) application of Sema3A or vehicle control. Under control conditions, growth cones remained spread out throughout the 15-min observation period (Fig. 2A). Upon exposure to Sema3A, collapse was evidenced by a reduction in growth cone area and partial or complete disappearance of lamellipodia and filopodia (Fig. 2B). Area was measured for the same growth cone over the experimental time and the change expressed as percent (Fig. 2E, F). Exposure to Sema3A over 15 min resulted in a 52.4% decrease in growth cone area compared to a non-significant 1.8% decrease for controls (for statistics, see Fig. 2F, bottom).

To determine whether Sema3A-induced growth cone collapse required activation of PLA_2 we pre-incubated DRG neurons with PLA_2 inhibitors for 15 min. This did not significantly change growth cone area (Fig. 2E). Because of the great diversity of candidate PLA_2s potentially involved we initiated these studies with an inhibitor for Groups IV and VI, $AACOCF_3$ (Ghomashchi et al., 1999), and a selective Group VI inhibitor, BEL, which is known to inhibit most Group VI activity in various cell types, including neurons (Wolf et al., 1995). In cultures pretreated with $AACOCF_3$, Sema3A failed to elicit growth cone collapse (Fig. 2F). In cultures pretreated with BEL, however, Sema3A induced full collapse like that seen without inhibitor. These results indicated that the PLA_2 activated by Sema3A most likely belonged to Group IV, a family of six different isoforms (Ghosh et al., 2006; Ohto et al., 2005). Because GIVA is selective for phospholipid substrates with AA in the sn-2 position [for review, see (Ghosh et al., 2006)] it was a strong candidate for Sema3A-

stimulated AA release. Pyrrolidine and Wyeth-1, which are structurally different, inhibit GIVA and GIVF (cPLA2ζ) highly selectively (Ghomashchi et al., 2001; Ghosh et al., 2007; Ni et al., 2006). Pyrrolidine is not known to have other targets. In cultures that had been pretreated with either compound and challenged with Sema3A, growth cones remained fully veiled and spread out (Fig. 2C and F). Collapse inhibition was highly significant statistically. Values for growth cone area change seemed to suggest an increase, but they were not significantly different from control. To ascertain that the inhibitors were not blocking steps down-stream of PLA_2 (such as lipoxygenase), we applied exogenous 12(S)-HETE to cultures pre-incubated with pyrrolidine. Growth cones collapsed normally, losing 35.6% of their area (Fig. 2D, F). It follows that selective inhibition of GIVA and/or GIVF blocks Sema3A-induced growth cone collapse.

Knock-down of GIVA prevents Sema3A-induced growth cone collapse

To confirm the PLA_2 inhibitor results and to discriminate between GIVA and GIVF, we used siRNA to silence PLA_2 expression. First we ascertained by western blot and immunocytochemistry that GIVA, the most likely isoform involved, was expressed in DRG growth cones (a mono-specific GIVF antibody was not available). GIVA PLA_2 (mass 85,200) migrates as a band of about 100kDa in SDS gels (Sharp et al., 1991). The western blot in Supplementary Figure S1A, probed with anti-GIVA PLA_2 (de Carvalho et al., 1993), was prepared with equal amounts of protein from: GIVA-expressing CHO cells (de Carvalho et al, 1993) as a positive control, fetal brain homogenate, low-speed supernatant of this homogenate, GCPs, and DRG cultures. All lanes exhibited a prominent doublet close to 100kDa, indicating that DRG neurons sprouting in culture and isolated CNS growth cones contain GIVA. Immunocytochemical analysis of DRG cultures confirmed the biochemical data (Supplementary Fig. S1B).

The selectivity of the rat GIVA-targeted siRNA (siGIVA) was determined in IMLFs, which express the PLA_2s GIVA, GIVB, GIVE and GIVF (Ghosh et al., 2007). Results of real-time qPCR experiments (Supplementary Fig. S2) show that siGIVA, a mixture of 3 siRNA duplexes (10 nM each, as used for the DRG neurons), reduced GIVA messenger RNA by over 80% without decreasing the other GIV PLA_2 messages. Even at 30 nM each, siGIVA did not affect these other messages. These results matched those of 100nM of a single siRNA targeting mouse PLA_2 GIVA and indicated that GIVA silencing was specific. We had previously targeted nuclear lamin (irrelevant to growth cone function), which activated the RNA interference mechanism but did not affect growth cone structure or function (Gatlin et al, 2006). Immunocytochemically we determined whether siGIVA (introduced with GFP as a marker) reduced expression of the enzyme. Supplementary Figures S1C and D show representative growth cones of a transfected (D; GFP-positive; green fluorescence not shown) and a non-transfected (C) neuron in the same culture (24h after transfection), labeled with anti-GIVA PLA_2. In all transfected growth cones examined there was a marked reduction in immunoreactivity compared to non-transfected controls (non-transfected growth cones, 23.8±6.0 arbitrary units; transfected growth cones, 9.6±4.9; $p \leq 0.003$; n=8). Thus, the siRNA markedly reduced GIVA levels in growth cones.

Neurons transfected with GFP alone or with scrambled siRNA plus GFP exhibited normal growth cone size and morphology. When exposed to Sema3A, these growth cones collapsed, losing 40.3% and 38.5%, respectively, of their total area. Before Sema3A application, growth cones transfected with siGIVA exhibited normal morphology (Fig. 3A, red arrow; Fig. 3B, 0 min), and their area was not significantly different from that of controls (Fig. 3C, top). When exposed to Sema3A, however, the collapse response was inhibited completely (red arrows in Fig. 3A; Fig. 3B, 15 min), while non-transfected growth cones in the same culture collapsed normally (white arrows in Fig. 3A). We also assessed whether the siGIVA-transfected, Sema3A-refractory growth cones responded to 12(S)-HETE, which signals

collapse down-stream of PLA_2. When siGIVA-transfected growth cones were exposed to this eicosanoid after 15 min of Sema3A challenge, they collapsed normally, like non-transfected controls (Fig. 3B, 30 min). Quantitative data (Fig. 3C) substantiate that GIVA PLA_2 is necessary for the Sema3A-induced collapse response of DRG growth cones.

Inhibition of PLA_2 activity affects growth cone turning

To address the question of whether PLA_2 activity was necessary for the complex function of growth cone turning, we tracked growth cone position over time in microgradients of Sema3A, when pyrrolidine was or was not present. This is shown as rosebud plots with a time resolution of 5 min (Fig. 4A). The origin of the rosebud plot (0 on the abscissa) represents the initial position of the growth cone. Results also are shown as the average final turning angles (Fig. 4B) and as cumulative distribution plots of turning angles (Fig. 4C). Under control conditions (micropipette filled with control medium) the growth cones continued to advance more or less in their initial direction of growth, and the resultant final turning angle was $-0.6° \pm 3.5°$ (Fig. 4B). When growth cones were exposed to microgradients of Sema3A, they turned away from the source [the micropipette tip (Fig. 4A; Sema3A)]. This resulted in repulsion with a final turning angle of $-13.2° \pm 5.4°$ ($p<0.035$; Fig. 4B) and a distribution plot mostly in the negative range (Fig. 4C). However, when pyrrolidine was present in the culture medium, the growth cones advanced toward the Sema3A source (Fig. 4A; Pyrrolidine+Sema3A). This resulted in a final turning angle of $+15.3° \pm 3.8°$. This attractive response was significantly different from control ($p<0.035$), Sema3A-only ($p \leq 0.0001$), and pyrrolidine+control values (which were indistinguishable from control). The result indicated that the GIVA inhibitor, pyrrolidine, switched Sema3A-induced growth cone repulsion to attraction.

Discussion

Our previous work described significant segments of the repellent-activated signaling pathway that triggers the disassembly of adhesion sites, an essential step in growth cone turning and collapse (Gatlin et al., 2006; Mikule et al., 2002; Mikule et al., 2003). Those studies also established that 12(S)-HETE generation is necessary and sufficient for growth cone detachment and collapse.

Sema3A stimulates the release of AA and 12(S)-HETE

12(S)-HETE is generated from free AA by 12/15-lipoxygenase (12/15-LO) and subsequent oxidation (Yamamoto et al., 1997). Thus, 12(S)-HETE synthesis requires PLA_2 activity. While 12/15-LO activity may be regulated to some degree, eicosanoid synthesis is believed to be controlled significantly by the supply of free AA (Yamamoto et al., 1997). Previous work in the laboratory has shown that the repellent, thrombin, increases free AA and 12(S)-HETE. However, the PLA_2 involved has not been identified, nor has its activation by Sema3A been examined. Because of the well-known rapid metabolism and reincorporation of AA into lipids, changes in AA levels are notoriously difficult to measure (Irvine, 1982). This is particularly true when the level of free AA under control conditions is high, as in the growth cone [see also (Negre-Aminou et al., 1996; Negre-Aminou and Pfenninger, 1993)] and other amoeboid systems, such as platelets (Kim et al., 1991), macrophages (Lefkowith et al., 1991; Leslie et al., 1988), and neutrophils (Burke et al., 1997; Fonteh, 2002)]. Only with the highly purified Sema3A-Fc chimera were we able to demonstrate a significant increase in AA release and, thus, PLA_2 stimulation. Our data also show that Sema3A significantly increased the level of the key eicosanoid, 12-HETE, over control conditions in DRG cultures.

GIVA PLA_2 is necessary for Sema3A-induced growth cone collapse

In these studies three inhibitors of intracellular PLA_2 blocked growth cone collapse, indicating that PLA_2 activity and the release of AA are necessary. These three PLA_2 inhibitors ($AACOCF_3$, pyrrolidine and Wyeth-1) all affect GIV PLA_2s, whereas BEL, which is selective for GVI PLA_2s, did not inhibit collapse. The results strongly suggest that GIVA and/or GIVF, rather than GVI PLA_2s, is/are involved in Sema3A-stimulated collapse signaling. Pyrrolidine is a highly selective inhibitor of both GIVA and GIVF, but it has a lower IC_{50} for GIVA (Ghosh et al., 2007). More significantly, GIVA is the only PLA_2 known to be selective for phospholipids with AA in the sn-2 position (Ghosh et al., 2006), making it an attractive candidate for releasing free AA upon Sema3A stimulation. Indeed, our loss-of-function experiments using siRNA showed that the GIVA isoform is necessary for Sema3A-stimulated growth cone collapse. While this does not exclude a possible role for GIVF, it indicates that GIVA is the main PLA_2 isoform responsible in DRG neurons.

Involvement of PLA_2 in neurite growth and chemotaxis has been reported by others as well (however, selectivity of some of the inhibitors used was suboptimal). Certain PLA_2 blockers inhibit the outgrowth of DRG neurons from adult mouse (Hornfelt et al., 1999) and frog (Edstrom et al., 1996). PLA_2 activity and its products (including AA) have also been shown to regulate filopodial length and number (Geddis et al., 2004). These effects may well be related to the role of PLA_2 in growth cone navigation described here. Inhibition of PLA_2 in *Dictyostelium discoideum* cell lines reduces chemotaxis, and it has been proposed that PLA_2 and its metabolites act in conjunction with phosphoinositide 3-kinase signaling to mediate chemotaxis (Chen et al., 2007; van Haastert et al., 2007). A genetic screen implicated a gene with homology to patatin-like PLA_2 in *Dictyostelium* chemotaxis (Chen et al., 2007). Interestingly, further analysis of this PLA_2 has shown structural similarity to GIVA PLA_2, as well as active-site sequence homology to GVI PLA_2 (Ghosh et al., 2006). These intriguing parallels between *Dictyostelium* and growth cones suggest a fundamental role for PLA_2 in regulating chemotaxis/adhesion processes.

GIVA PLA_2 is necessary for Sema3A-induced growth cone turning

Uniform bath application of a repellent results in growth cone collapse. In contrast, application of a repellent gradient, which resembles the situation *in vivo* more closely, affects the growth cone asymmetrically and deflects its advance. When growth cones pre-incubated with pyrrolidine were exposed to a Sema3A gradient, repulsion was inhibited. It would have been of great interest to repeat these experiments with siGIVA, but the inherent technical challenges, combined with relatively low transfection efficiency, made such studies unrealistic. However, the high selectivity of pyrrolidine and the fact that it did not just block repulsion but switched repulsion to attraction further stressed the specificity of the effect and the importance of the enzyme in the growth cone's turning response. Remarkably, this switch is consistent with our earlier observation that Sema3A-induced repulsion changed to attraction when growth cones expressed phosphorylation-deficient MARCKS, a protein downstream in the pathway (Gatlin et al., 2006). The attenuation of growth cone repulsion by GIVA inhibition can be explained by the reduced generation of 12(S)-HETE, which, in turn, minimizes phosphorylation-dependent dissociation of MARCKS from the plasma membrane (Fig. 5). As a result existing adhesion sites remain fixed, and asymmetric growth cone detachment cannot occur. The switch to Sema3A-induced attraction caused by the PLA_2 inhibitor is more difficult to explain. The possibility that the conditioned control and/or Sema3A media contained an attractant whose function became detectable only in the presence of pyrrolidine seemed unlikely because the pyrrolidine+control experiment did not show attraction (Sema3A-Fc became available only late in the course of these experiments and was not used). Interestingly, a number of other studies have shown the switch from

repulsion to attraction when components of Sema3A-signaling were inhibited (Castellani et al., 2002; Castellani and Rougon, 2002; Gatlin et al., 2006; Song et al., 1998).

Conclusions

Recently developed, selective PLA_2 inhibitors, together with expression silencing, have enabled us to add a further element, GIVA PLA_2, to the pathway that links Sema3A-triggered signaling to growth cone turning and collapse. As we have shown previously, turning and collapse require repellent-triggered detachment of adhesions. Together with those earlier data (de la Houssaye et al., 1999; Gatlin et al., 2006; Mikule et al., 2002; Mikule et al., 2003), we can now develop the model shown in Figure 5. In this model, Sema3A binding to its receptor (NP-1) stimulates GIVA PLA_2, releasing free AA. Free AA is converted by 12/15-LO into 12(S)-HETE [and smaller amounts of 15(S)-HETE and 5(S)-HETE]. 12(S)-HETE [and 15(S)-HETE] activates PKCε directly which, in turn, phosphorylates MARCKS. While non-phosphorylated MARCKS serves as a stabilizer of growth cone adhesions, phospho-MARCKS dissociates from the membrane and moves into the cytosol. Release of MARCKS from adhesion sites causes their destabilization and detachment. Uniform growth cone detachment leads to growth cone collapse, whereas asymmetric detachment in a gradient of Sema3A causes turning to the attached side further away from the gradient source, i.e., repulsion. This occurs in conjunction with modulation of the growth cone's cytoskeleton. The steps marked by an asterisk in Figure 5 have been shown to be necessary for growth cone turning and collapse, and those with the pound sign have been shown to be sufficient for collapse. Overlap between the signaling of thrombin and Sema3A (de la Houssaye et al., 1999; Mikule et al., 2002), which operate through very different receptor types, and the fact that many of the biochemical data were obtained from CNS growth cones suggest that this pathway may be functional in conjunction with a variety of repellents and in CNS neurons as well.

Supplementary Material

Refer to Web version on PubMed Central for supplementary material.

Acknowledgments

The authors wish to express their gratitude to Charis Uhlson and Dr. Simona Zarini, for performing the mass-spectrometric determinations of arachidonic acid and eicosanoids, and Dr. Misoo Ellison, for her expert help with the statistical analyses. Further appreciation goes to the laboratory of Dr. Nicholas Seeds, University of Colorado School of Medicine, for help with the immunocytochemical experiments, and to Hee Jung Lee, National Jewish Health, for assistance with the qPCR. We wish to acknowledge the generous gifts of Wyeth-1, from M. Gelb, University of Washington, Seattle, and of HEK293 cells secreting Sema3A, from M. Tessier-Lavigne. This work was supported by National Institutes of Health (NIH) grants R01 NS041029 and R01 NS061940 (awarded to K.H.P.), NIH National Research Service Award F31 NS48710 (to S.D.S.), NIH grants HL34303 and HL61378 (to C.C.L.), and NIH Health Lipid Maps grant GM069338 (to R.C.M.).

Abbreviations

AA	arachidonic acid
AACOCF$_3$	arachidonyltrifluoromethyl ketone
ANOVA	Analysis of Variance
BEL	bromoenol lactone
BSA	bovine serum albumin
DRG	dorsal root ganglion

FDR	False Discovery Rate
GCP	growth cone particle
GIV	group IV phospholipase A_2
GVI	group VI phospholipase A_2
5(S)-HETE	5(S)-hydroxyeicosatetraenoic acid
12(S)-HETE	12(S)-hydroxyeicosatetraenoic acid
15(S)-HETE	15(S)-hydroxyeicosatetraenoic acid
IMLF	immortalized mouse lung fibroblast
K-W	Kruskal-Wallis test
12/15-LO	12/15-lipoxygenase
MARCKS	myristoylated, alanine-rich C-kinase substrate
NGF	nerve growth factor
NP-1	neuropilin-1
pCEP4	supernatant of HEK293 cells transfected with empty vector
PI3K	phosphoinositide 3-kinase
PKC	protein kinase C
PLA_2	phospholipase A_2
pyrrolidine	N-{(2S,4R)-4-(Biphenyl-2-ylmethyl-isobutyl-amino)-1-[2-(2,4-difluorobenzoyl)-benzoyl]-pyrrolidin-2-ylmethyl}-3-[4-(2,4-dioxothiazolidin-5-ylidenemethyl)-phenyl]-acrylamide
q-PCR	quantitative polymerase chain reaction
Sema3A	semaphorin 3A
siRNA	small interfering RNA

References

Burke JR, Davern LB, Gregor KR, Tramposch KM. Leukotriene B4 stimulates the release of arachidonate in human neutrophils via the action of cytosolic phospholipase A2. Biochim Biophys Acta. 1997; 1359:80–88. [PubMed: 9398088]

Castellani V, De Angelis E, Kenwrick S, Rougon G. Cis and trans interactions of L1 with neuropilin-1 control axonal responses to semaphorin 3A. Embo J. 2002; 21:6348–6357. [PubMed: 12456642]

Castellani V, Rougon G. Control of semaphorin signaling. Curr Opin Neurobiol. 2002; 12:532–541. [PubMed: 12367632]

Chen L, Iijima M, Tang M, Landree MA, Huang YE, Xiong Y, Iglesias PA, Devreotes PN. PLA2 and PI3K/PTEN pathways act in parallel to mediate chemotaxis. Dev Cell. 2007; 12:603–614. [PubMed: 17419997]

De Carvalho MS, mccormack FX, Leslie CC. The 85-kda, arachidonic acid-specific phospholipase A2 is expressed as an activated phosphoprotein in Sf9 cells. Arch Biochem Biophys. 1993; 306:534–540. [PubMed: 8215460]

De la Houssaye BA, Mikule K, Nikolic D, Pfenninger KH. Thrombin-induced growth cone collapse: involvement of phospholipase A(2) and eicosanoid generation. J Neurosci. 1999; 19:10843–10855. [PubMed: 10594066]

Edstrom A, Briggman M, Ekstrom PA. Phospholipase A2 activity is required for regeneration of sensory axons in cultured adult sciatic nerves. J Neurosci Res. 1996; 43:183–189. [PubMed: 8820966]

Fan J, Raper JA. Localized collapsing cues can steer growth cones without inducing their full collapse. Neuron. 1995; 14:263–274. [PubMed: 7857638]

Fonteh AN. Differential effects of arachidonoyl trifluoromethyl ketone on arachidonic acid release and lipid mediator biosynthesis by human neutrophils. Evidence for different arachidonate pools. Eur J Biochem. 2002; 269:3760–3770. [PubMed: 12153573]

Gatlin JC, Estrada-Bernal A, Sanford SD, Pfenninger KH. Myristoylated, alanine-rich C-kinase substrate phosphorylation regulates growth cone adhesion and pathfinding. Mol Biol Cell. 2006; 17:5115–5130. [PubMed: 16987960]

Geddis MS, Tornieri K, Giesecke A, Rehder V. PLA2 and secondary metabolites of arachidonic acid control filopodial behavior in neuronal growth cones. Cell Motil Cytoskeleton. 2004; 57:53–67. [PubMed: 14648557]

Ghomashchi F, Loo R, Balsinde J, Bartoli F, Apitz-Castro R, Clark JD, Dennis EA, Gelb MH. Trifluoromethyl ketones and methyl fluorophosphonates as inhibitors of group IV and VI phospholipases A(2): structure-function studies with vesicle, micelle, and membrane assays. Biochim Biophys Acta. 1999; 1420:45–56. [PubMed: 10446289]

Ghomashchi F, Stewart A, Hefner Y, Ramanadham S, Turk J, Leslie CC, Gelb MH. A pyrrolidine-based specific inhibitor of cytosolic phospholipase A(2)alpha blocks arachidonic acid release in a variety of mammalian cells. Biochim Biophys Acta. 2001; 1513:160–166. [PubMed: 11470087]

Ghosh M, Loper R, Ghomashchi F, Tucker DE, Bonventre JV, Gelb MH, Leslie CC. Function, activity, and membrane targeting of cytosolic phospholipase A(2)zeta in mouse lung fibroblasts. J Biol Chem. 2007; 282:11676–11686. [PubMed: 17293613]

Ghosh M, Tucker DE, Burchett SA, Leslie CC. Properties of the Group IV phospholipase A2 family. Prog Lipid Res. 2006; 45:487–510. [PubMed: 16814865]

Hall A. Rho gtpases and the actin cytoskeleton. Science. 1998; 279:509–514. [PubMed: 9438836]

Hornfelt M, Ekstrom PA, Edstrom A. Involvement of axonal phospholipase A2 activity in the outgrowth of adult mouse sensory axons in vitro. Neuroscience. 1999; 91:1539–1547. [PubMed: 10391457]

Irvine RF. How is the level of free arachidonic acid controlled in mammalian cells? Biochem J. 1982; 204:3–16. [PubMed: 6810878]

Kim DK, Kudo I, Inoue K. Purification and characterization of rabbit platelet cytosolic phospholipase A2. Biochim Biophys Acta. 1991; 1083:80–88. [PubMed: 2031941]

Kim J, Blackshear PJ, Johnson JD, Mclaughlin S. Phosphorylation reverses the membrane association of peptides that correspond to the basic domains of MARCKS and neuromodulin. Biophys J. 1994; 67:227–237. [PubMed: 7918991]

Lauffenburger DA, Horwitz AF. Cell migration: a physically integrated molecular process. Cell. 1996; 84:359–369. [PubMed: 8608589]

Lefkowith JB, Rogers M, Lennartz MR, Brown EJ. Essential fatty acid deficiency impairs macrophage spreading and adherence. Role of arachidonate in cell adhesion. J Biol Chem. 1991; 266:1071–1076. [PubMed: 1985935]

Leslie CC, Voelker DR, Channon JY, Wall MM, Zelarney PT. Properties and purification of an arachidonoyl-hydrolyzing phospholipase A2 from a macrophage cell line, RAW 264.7. Biochim Biophys Acta. 1988; 963:476–492. [PubMed: 3143418]

Liu BP, Strittmatter SM. Semaphorin-mediated axonal guidance via Rho-related G proteins. Curr Opin Cell Biol. 2001; 13:619–626. [PubMed: 11544032]

Livak KJ, Schmittgen TD. Analysis of relative gene expression data using real-time quantitative PCR and the 2(-Delta Delta C(T)) Method. Methods. 2001; 25:402–408. [PubMed: 11846609]

Lohof AM, Quillan M, Dan Y, Poo MM. Asymmetric modulation of cytosolic camp activity induces growth cone turning. J Neurosci. 1992; 12:1253–1261. [PubMed: 1372932]

Lohse K, Helmke SM, Wood MR, Quiroga S, de la Houssaye BA, Miller VE, Negre-Aminou P, Pfenninger KH. Axonal origin and purity of growth cones isolated from fetal rat brain. Brain Res Dev Brain Res. 1996; 96:83–96.

Luo Y, Raible D, Raper JA. Collapsin: a protein in brain that induces the collapse and paralysis of neuronal growth cones. Cell. 1993; 75:217–227. [PubMed: 8402908]

Mikule K, Gatlin JC, de la Houssaye BA, Pfenninger KH. Growth cone collapse induced by semaphorin 3A requires 12/15-lipoxygenase. J Neurosci. 2002; 22:4932–4941. [PubMed: 12077190]

Mikule K, Sunpaweravong S, Gatlin JC, Pfenninger KH. Eicosanoid activation of protein kinase C epsilon: involvement in growth cone repellent signaling. J Biol Chem. 2003; 278:21168–21177. [PubMed: 12665507]

Murakami M, Kudo I. Secretory phospholipase A2. Biol Pharm Bull. 2004; 27:1158–1164. [PubMed: 15305013]

Negre-Aminou P, Nemenoff RA, Wood MR, de la Houssaye BA, Pfenninger KH. Characterization of phospholipase A2 activity enriched in the nerve growth cone. J Neurochem. 1996; 67:2599–2608. [PubMed: 8931495]

Negre-Aminou P, Pfenninger KH. Arachidonic acid turnover and phospholipase A2 activity in neuronal growth cones. J Neurochem. 1993; 60:1126–1136. [PubMed: 8436962]

Ni Z, Okeley NM, Smart BP, Gelb MH. Intracellular actions of group IIA secreted phospholipase A2 and group IVA cytosolic phospholipase A2 contribute to arachidonic acid release and prostaglandin production in rat gastric mucosal cells and transfected human embryonic kidney cells. J Biol Chem. 2006; 281:16245–16255. [PubMed: 16603549]

Ohto T, Uozumi N, Hirabayashi T, Shimizu T. Identification of novel cytosolic phospholipase A(2)s, murine cpla(2){delta}, {epsilon}, and {zeta}, which form a gene cluster with cpla(2){beta}. J Biol Chem. 2005; 280:24576–24583. [PubMed: 15866882]

Pfenninger KH, Ellis L, Johnson MP, Friedman LB, Somlo S. Nerve growth cones isolated from fetal rat brain: subcellular fractionation and characterization. Cell. 1983; 35:573–584. [PubMed: 6652678]

Pfenninger KH, Maylie-Pfenninger MF. Lectin labeling of sprouting neurons. I. Regional distribution of surface glycoconjugates. J Cell Biol. 1981; 89:536–546. [PubMed: 7251664]

Sanford SD, Gatlin JC, Hokfelt T, Pfenninger KH. Growth cone responses to growth and chemotropic factors. Eur J Neurosci. 2008

Schaloske RH, Dennis EA. The phospholipase A2 superfamily and its group numbering system. Biochim Biophys Acta. 2006; 1761:1246–1259. [PubMed: 16973413]

Sharp JD, White DL, Chiou XG, Goodson T, Gamboa GC, Mcclure D, Burgett S, Hoskins J, Skatrud PL, Sportsman JR, et al. Molecular cloning and expression of human Ca(2+)-sensitive cytosolic phospholipase A2. J Biol Chem. 1991; 266:14850–14853. [PubMed: 1869522]

Song H, Ming G, He Z, Lehmann M, Mckerracher L, Tessier-Lavigne M, Poo M. Conversion of neuronal growth cone responses from repulsion to attraction by cyclic nucleotides. Science. 1998; 281:1515–1518. [PubMed: 9727979]

Stewart A, Ghosh M, Spencer DM, Leslie CC. Enzymatic properties of human cytosolic phospholipase A(2)gamma. J Biol Chem. 2002; 277:29526–29536. [PubMed: 12039969]

Suter DM, Forscher P. Substrate-cytoskeletal coupling as a mechanism for the regulation of growth cone motility and guidance. J Neurobiol. 2000; 44:97–113. [PubMed: 10934315]

Thelen M, Rosen A, Nairn AC, Aderem A. Regulation by phosphorylation of reversible association of a myristoylated protein kinase C substrate with the plasma membrane. Nature. 1991; 351:320–322. [PubMed: 2034276]

Towbin H, Staehelin T, Gordon J. Electrophoretic transfer of proteins from polyacrylamide gels to nitrocellulose sheets: procedure and some applications. Proc Natl Acad Sci U S A. 1979; 76:4350–4354. [PubMed: 388439]

Van Haastert PJ, Keizer-Gunnink I, Kortholt A. Essential role of PI3-kinase and phospholipase A2 in Dictyostelium discoideum chemotaxis. J Cell Biol. 2007; 177:809–816. [PubMed: 17535967]

Wolf MJ, Izumi Y, Zorumski CF, Gross RW. Long-term potentiation requires activation of calcium-independent phospholipase A2. FEBS Lett. 1995; 377:358–362. [PubMed: 8549755]

Yamamoto S, Takahashi Y, Hada T, Hagiya H, Suzuki H, Reddy GR, Ueda N, Arakawa T, Nakamura M, Matsuda S, Taketani Y, Yoshimoto T, Azekawa T, Morita Y, Ishimura K, Arase S, Glasgow

WC, Brash AR, Anton M, Kuhn H. Mammalian arachidonate 12-lipoxygenases. Adv Exp Med Biol. 1997; 400A:127–131. [PubMed: 9547547]

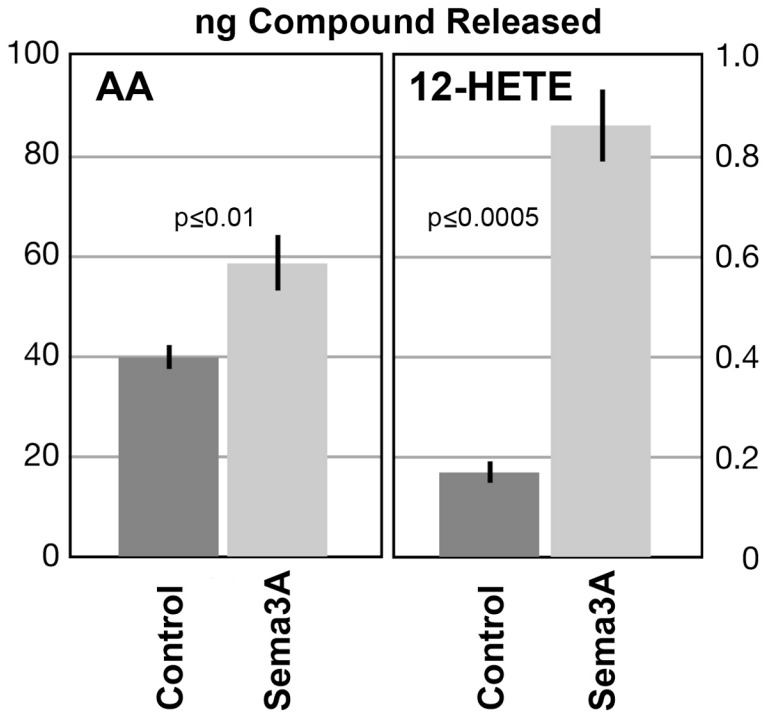

Figure 1.

Release of AA and 12-HETE from growing DRG neurons in culture, with and without Sema3A-Fc challenge (mean ng compound ± SEM). Supernatants of cultures of dissociated DRG neurons (equal cell numbers plated on laminin) were analyzed mass-spectrometrically. Control, 6 min challenge with vehicle; Sema3A, 6 min challenge with Sema3A. n=4 for AA; n=3 for 12-HETE.

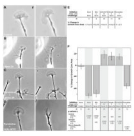

Figure 2.

Effect of PLA_2 inhibition on Sema3A-induced growth cone collapse. Growth cones of DRG neurons in explant cultures (on laminin) were exposed by bath application to either vehicle (control), Sema3A, or 12(S)-HETE, with or without pyrrolidine present. **A and B,** phase contrast micrographs of growth cones before (left panel) or 15 min after (right panel) bath application of either control medium or Sema3A. **C and D,** growth cones pre-incubated (15 min) with 1μM pyrrolidine, before (left panel) and 15 min after (right panel) bath application of either Sema3A or 10^{-8}M 12(S)-HETE. Scale bar 10μm. **E,** growth cone area changes (mean % change ± SEM) over 15min in the presence of PLA_2 inhibitors, without Sema3A challenge. These values are not significantly different from that for control incubation. **F,** quantitative analysis of growth cone collapse in the presence of various PLA_2 inhibitors. Results are expressed as mean % change in growth cone area ± SEM, measured at t=0 min and t=15 min after onset of challenge. The inhibitor and concentration used, the challenge, and the n values are indicated below each condition, as are the p values when contrasting individual measurements. Because the distribution of values was marginally normal, p values are shown for both parametric (ANOVA, FDR) and non-parametric (K-W, Dunn's procedure) statistical analyses. The overall p value was <0.0001 for both analyses. Grey shading has been added to facilitate reading of the graph.

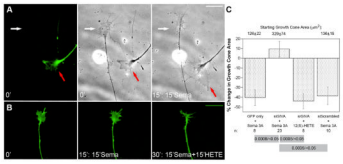

Figure 3.

Effect of silencing GIVA PLA_2 expression on Sema3A-induced growth cone collapse. All experiments included a GFP-encoding plasmid to identify transfected cells (dissociated DRG neurons). **A,** the first panel shows GFP labeling of the growth cone of a transfected neuron (red arrow). The white arrow points at a growth cone of a non-transfected neuron. The second and third panels show phase contrast micrographs of the first frame (0 min exposure to Sema3A) and of the same growth cones after 15 min of Sema3A exposure, respectively. Note enlargement of the transfected growth cone versus area reduction of the non-transfected growth cone. Scale bar 10μm. **B,** GFP labeling of the same transfected growth cone at three different experimental points: t=0 (first panel); 15 min Sema3A challenge (second panel); and t=30 min, i.e., 15 min Sema3A treatment followed by 15 min 10^{-8}M 12(S)-HETE challenge (third panel). Note that reduction in growth cone size occurs not after Sema3A, but after subsequent 12(S)-HETE challenge. Scale bar 10μm. **C,** quantitative analysis of growth cone area after transfection and challenge with either Sema3A or 12(S)-HETE. The actual growth cone sizes (in μm^2 ± SEM; for n values, see bottom of the graph) at the onset of the challenge are indicated on the top. While the siGIVA growth cones were more variable in size, on average they were not significantly different from those from GFP-only and siScrambled neurons. These same growth cones were subsequently challenged. To assess challenge-induced change, growth cone areas were measured at t=0 min and t=15 min after onset of the challenge. Results are expressed as mean % change in growth cone area ± SEM. Values for n are indicated below the graph. Because the distribution of data was marginally normal, p values from both parametric (ANOVA, FDR) and non-parametric (K-W, Dunn's procedure) statistical analyses are included in the grey rules whose ends designate the individual measurements to be contrasted (p ANOVA/p K-W). The overall p value was <0.0001 in both analyses.

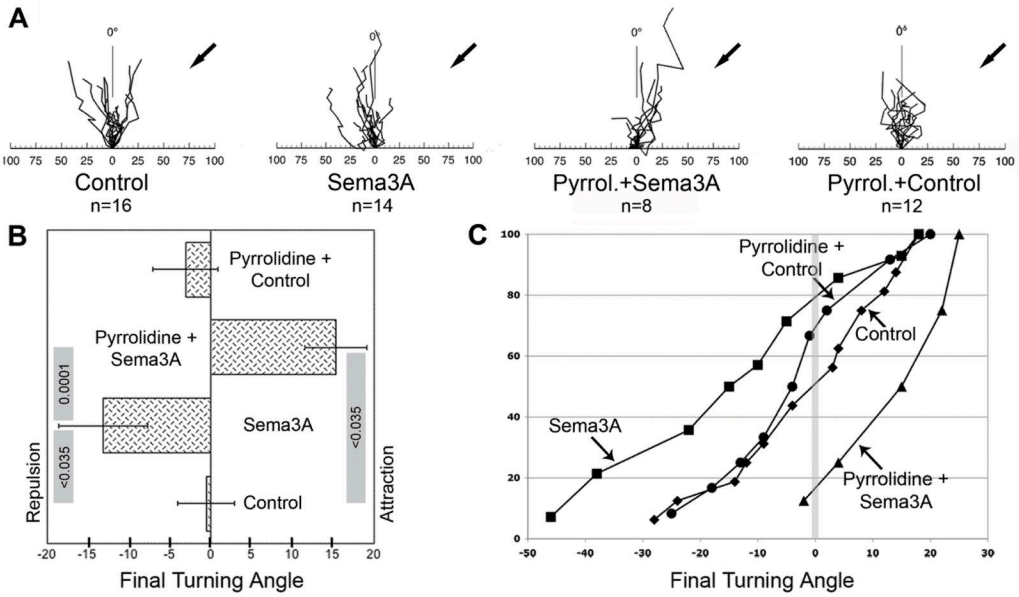

Figure 4.

Effect of GIVA PLA_2 inhibition on Sema3A-induced growth cone turning. Growth cones of DRG neurons (explants on laminin) were exposed to gradients of control medium or Sema3A in the presence or absence of 1μM pyrrolidine. **A,** rosebud plots of axonal responses. Plots illustrate growth cone translocation during gradient exposure for 1 h, shown at a time resolution of 5 min. Arrows mark the position of the micropipette tip. The abscissa indicates distance in micrometers, and the ordinate marks 0° in an arc from −90° to +90°. **B,** final turning angles (means ± SEM) in response to gradients of either control medium or Sema3A, with or without pyrrolidine present in the culture media. p values are shown in the grey rules whose ends designate the individual measurements to be contrasted (ANOVA, FDR). The overall p value was <0.0009. **C,** cumulative distribution plots of turning angles in response to (from left to right) Sema3A, Pyrrolidine + Control, Control, and Pyrrolidine + Sema3A. The vertical grey line marks the 0° turning angle.

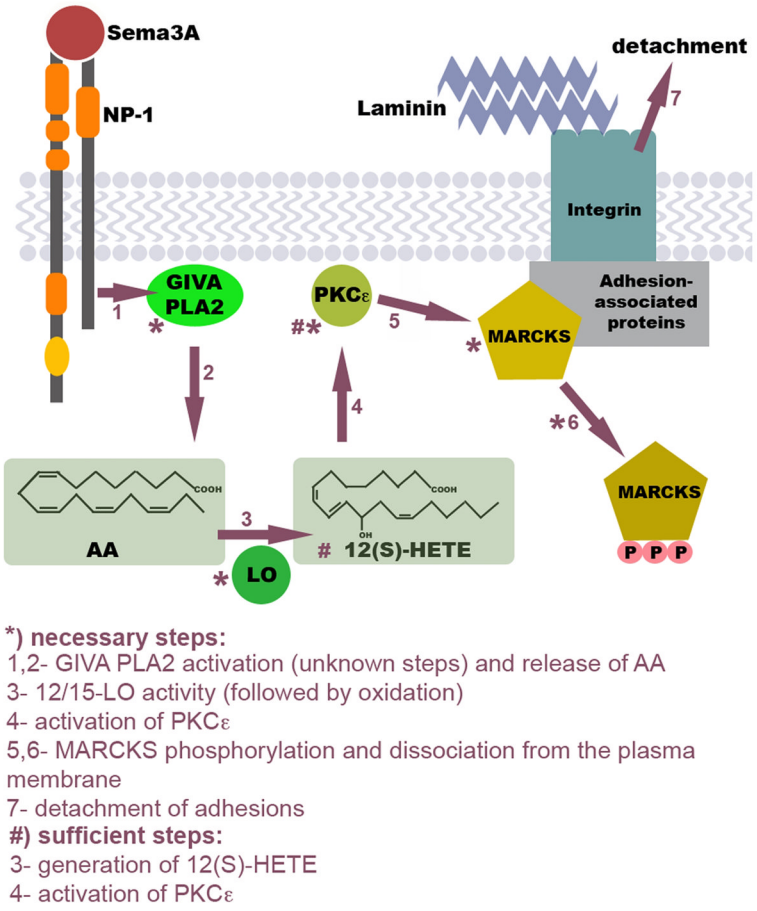

Figure 5.

Model of the Sema3A-activated signaling pathway that triggers adhesion site disassembly. Via currently unknown steps (1) the Sema3A receptor (NP-1, neuropilin-1) activates GIVA PLA_2. The released AA (2) is converted primarily to 12(S)-HETE by 12/15-LO (3), which selectively activates PKCε (4). PKCε phosphorylation of adhesion-associated MARCKS (5) triggers its dissociation from the plasma membrane (6) and adhesion site disassembly, which causes growth cone detachment (7). If this response is localized it results in growth cone repulsion; if it is generalized, it triggers growth cone collapse. Steps that are known to be necessary and/or sufficient are indicated. This model is supported by the data presented here and by previous publications (see Discussion).